Springer

KSME

Journal of Mechanical Science and Technology 30 (12) (2016) 5405~5412
www.springerlink.com/content/1738-494x(Print)/1976-3824(Online)
DOI 10.1007/s12206-016-1108-3

Numerical and experimental analysis of coupled transverse and longitudinal vibration of a marine propulsion shaft †

Qianwen Huang[1,2], Xinping Yan[1,3,*], Yikun Wang[2], Cong Zhang[1] and Yong Jin[1]

[1]*Reliability Engineering Institute, School of Energy and Power Engineering, Wuhan University of Technology, Wuhan, 430063, China*
[2]*Faculty of Engineering and the Environment, University of Southampton, Southampton, SO17 1BJ, United Kingdom*
[3]*National Engineering Research Center for Water Transport Safety, Wuhan University of Technology, Wuhan, 430063, China*

(Manuscript Received March 21, 2016; Revised June 17, 2016; Accepted July 8, 2016)

Abstract

An appropriate assessment of the dynamic behavior of marine propulsion shaft in ships is essential to enable optional delivery of power to the propeller and to minimize unnecessary vibration. Various vibrations coupling with each other can significantly influence the dynamical behavior of the shaft and threaten the reliability of ships. This paper presents a finite element analysis model with multiple constraint conditions to analyze the coupled transverse and longitudinal vibrations of a marine propulsion shaft. Based on this model, in addition to the coupled natural frequencies of each direction, the maximum acceleration are also determined. Furthermore, the simulation of an idling and loading vibration analysis is discussed and validated against experimental results, over a range of rotational speeds. The output of numerical simulation is found to agree with the corresponding results from experimental tests. Finally, an accurate and applicative FEA model for coupled transverse-longitudinal vibration of shaft has been obtained.

Keywords: Coupled transverse-longitudinal vibration; Marine propulsion shaft; Finite element analysis; Numerical simulation; Experiment setup

1. Introduction

The main engine functions as the heart part of a ship and plays an important role in its reliability. The propulsion shaft connects to main engine and transmits its torque to the propeller to promote the operation of the ship [1]. As is known, the propulsion shaft experiences different exciting forces during the operation. Torsional vibration, induced by the pulsing torque of the engine, variable propeller output and the torsional elasticity of power transmission system is considered to be much unsafe [2]. Longitudinal vibration, attributed to unsteady propeller thrust, increases the relative motion between fixed and rotating parts, thus cause wear of thrust bearings [3]. Transverse vibration, attributed to the imbalance of the rotating part of the shaft system and the periodic motion of alternating bending deformation caused by the propeller in the non-uniform flow field [4]. Moreover, the coupled forms of the abovementioned vibrations are undesirable and have led to numerous shaft failures [5].

Coupled vibrations, such as coupled torsional, longitudinal and transverse vibrations of the propeller shaft, as well as shaft and hull-deformation coupled vibration are emerging topics in the ship research field over the past decades [6]. During navigations, ships are usually perturbed by waves, wind and many other exciting forces in different forms. As a result, vibration responses will be excited in different directions simultaneously. Moreover, the pulsation of cycle work in the main engine and the non-uniformity of the propeller working area will cause extremely complex exciting forces. These external and internal incentives couple with each other and will influence the reliability of the propulsion shaft [7]. The mechanism of the coupled vibrations is that each point on the shaft generates a response not only in the direction of the disturbing force but also in other directions.

As an indispensable factor, the issue of vibrations should be considered in the initial design process, in order to avoid addition cost for maintenance and repair. It is considered important to address those potential problems in terms of the minimal technology available at the design stage [8]. Early investigations only considered the shaft system and employed simple models, such as transfer matrix method [9] to analyze individual vibration in various directions of the shaft. These models are fundamental to describe a particular shaft vibration but not sufficient to address a coupled shaft vibration scenario. Recently, investigations were conducted with more complicated models, for example using energy method [10], system matrix method [11] or mode synthesis method [12] consisting of the

*Corresponding author. Tel.: +86 27 86549879, Fax.: +86 27 86549879
E-mail address: xpyan@whut.edu.cn
† Recommended by Associate Editor Ohseop Song

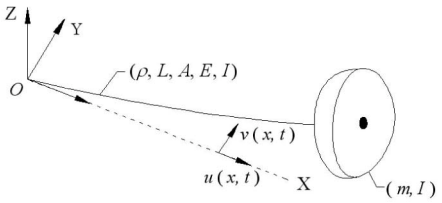

Fig. 1. The schematic of the beam (here, L, A and I denote the length of the beam, cross-sectional area and moment of inertia, respectively. ρ, E and m denote the density, elastic modulus and mass, respectively. And $u(x, t)$ and $v(x, t)$ denote the longitudinal and transverse deformation).

interaction of various directions of the propeller shaft. Meanwhile, experimental research regarding shaft dynamics and vibration control has also been carried out [13].

Nevertheless, few investigations focus on the coupled transverse and longitudinal vibrations. The disadvantage of the analytical models in the literature is the lack of flexibility to deal with vibrations containing complicated coupling effects at rotational speeds [14]. Moreover, the previous research indicated that the shaft deflects severely due to the hull deformation by a comparison of shaft in dry dock and service [15, 16]. The vibration study for loading condition is thus extremely necessary. Therefore, the most ideal method is to be able to predict the dynamical performance with the abovementioned factors as well as to be convenient to use in a practical analysis. In view of this, a finite element method with coupling constraint for different rotational speeds is therefore preferable in studying shaft vibrations, from which a good estimation of the coupled vibration behavior can be obtained.

In this paper, an experimental setup of coupled transverse and longitudinal vibration of a marine propulsion shaft was introduced. And a Finite element analysis (FEA) model focusing on the abovementioned vibrations was developed. Thus, a feasibility study of the dynamical performance due to the variation of rotational speed was presented. The coupled natural frequencies and maximum acceleration were investigated through experiment and simulation. It was reported that the hull deformation effects the shaft vibration seriously. During the operation of ships, the shaft will always affected by the hull deformations. Therefore, both idling and loading conditions were considered. The results under loading condition were discussed to study the effect of hull deformation on the shaft vibration. Moreover, the experimental and simulated results were compared to validate the FEA model.

2. Equations of motion

The shaft can be model as an Euler beam with a mass payload, as shown in Fig. 1, which is equivalent to a cantilever beam with its mass center away from the centerline [17].

According to the theory of material mechanics and the stress-strain relationship in elastic mechanics, the principal strain ε_x is:

$$\varepsilon_x = \frac{\partial U}{\partial x} + \frac{1}{2}(\frac{\partial V}{\partial x})^2 = \frac{\partial u}{\partial x} - y\frac{\partial^2 v}{\partial x^2} + \frac{1}{2}(\frac{\partial v}{\partial x})^2 \tag{1}$$

where U and V denote the longitudinal and transverse deformation regarding time, X-axial and Y-axial (shown in Fig. 1). u and v denote the abovementioned deformation component regarding time and X-axial.

According to the Hooke's law, the principal stress is $\sigma_x = E\varepsilon_x$ and the theorem of kinetic energy $E_k = mv^2/2$, the strain energy (PE) and kinetic energy (KE) of the shaft can be expressed as the following Eqs. (2) and (3) [18]:

$$PE = \frac{1}{2}\int_l [EA(\frac{\partial u}{\partial x} + \frac{1}{2}\frac{\partial^2 v}{\partial x^2})^2 + EI(\frac{\partial v}{\partial x})^4]dx \tag{2}$$

$$KE = \frac{1}{2}\int_l \{\rho[(\frac{\partial u}{\partial t})^2 + (\frac{\partial v}{\partial t})^2] + \rho I(\frac{\partial^2 v}{\partial x \partial t})^2\}dx\,. \tag{3}$$

When the beam is under an external fore, the work is $W = Fs$ (here, s is the displacement produced by the force). Defining the longitudinal force as $N_x \sin\omega_u t$ and transverse force as $F_z \sin\omega_v t$, the external energy induced by longitudinal force (U_u) and transverse force (U_v) can be calculated respectively as:

$$U_u = \frac{1}{2}\int_l N_X \sin\omega_u t du \tag{4}$$

$$U_v = \frac{1}{2}\int_l F_Z \sin\omega_v t dv \tag{5}$$

where ω_u and ω_v denote the frequencies of the external longitudinal and transverse forces, respectively.

Combining the strain energy in Eq. (2) and the kinetic energy in Eq. (3), a Lagrange function L of time for the shaft can be established. Similarly, combining the work by longitudinal force in Eq. (4) and transverse force in Eq. (5), a Lagrange function W of time for the shaft can be established. According to the virtual displacement formula, the following equations can be obtained:

$$\int_1^f Ldt = \int_1^f (KE - PE)dt \tag{6}$$

$$\int_1^f Wdt = \int_1^f (U_u + U_v)dt\,. \tag{7}$$

Adopting the subsection integral method based on the Hamilton principle: $\delta\int_1^f (W - L)dt = 0$, Eqs. (6) and (7) can be presented as:

$$\begin{aligned}\delta\int_1^f (W-L)dt = \delta\int_1^f \{\int_l (-EAu''\delta u dx - EIv''\delta v dx) - \\ [-\rho A(\ddot{u}\delta u dx + \ddot{v}\delta v dx) + \rho I\ddot{v}''\delta v dx + \\ EA(u' + v'^2/2)'(\delta u dx + v'\delta v dx) - (EIv'')''\delta v dx]\}dt\end{aligned} \tag{8}$$

where u'' and v'' are the second order derivatives of longitudinal and transverse displacements along X-axial, $\ddot{u}$ and $\ddot{v}$ are the second order derivatives of longitudinal and transverse

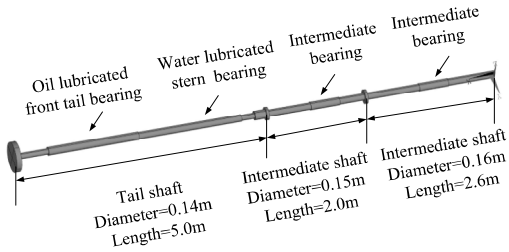

Fig. 2. The schematic of the tested shaft system.

displacements versus time, respectively.

Thus, according to the Principle of Hamilton, the coupled vibration equation in Eq. (8) can be written as:

$$-\rho A\ddot{u}+EA(u'+\frac{1}{2}v'^2)'=-EAu'' \tag{9}$$

$$-\rho A\ddot{v}-(EIv'')''+\rho I\ddot{v}''+[EA(u'+\frac{1}{2}v'^2)']v'=-EIv''. \tag{10}$$

Since this paper focuses on the coupled vibrations of an Euler beam, the influences of shear deformation and moment of inertia are not considered. Assuming the transverse and longitudinal forces are zero, Eqs. (9) and (10) represent the coupled longitudinal and transverse vibrations of a cantilever beam without external forces. It can be seen that the deformation in the longitudinal and transverse directions will interact during the vibration.

3. Experiment setup

To verify the deduced coupled equations Eqs. (9) and (10), the vibrations of a propulsion shaft were experimentally measured. The tested shaft system, schematically illustrated in Fig. 2, mainly consisted of the frequency conversion motor, the decelerator, the thrust and support bearings, the propulsion shaft, the foundation and the base. Besides, it was equipped with lubrication system, hydraulic loading system and state monitoring system. The dimensions of the shafts are also shown in Fig. 2.

The base was mounted on the foundation, with the propulsion shafts and bearings fixed on it. The propulsion shaft system contained two intermediate shafts and a tail shaft, with a hydraulic coupling connecting between each shafts with. The two intermediate shafts were supported by an intermediate bearing, while the tail shaft was supported by a water lubricated stern bearing and an oil lubricated front tail bearing, as shown in Fig. 3.

The duration of each experiment was set to be 10 seconds, and the results for stable rotation for 1 second was selected for data analysis. During the experiment, the harmonic and transient responses of the transverse and longitudinal vibration were obtained simultaneously. The response data with idling and loading condition for each rotational speed were extracted and recorded.

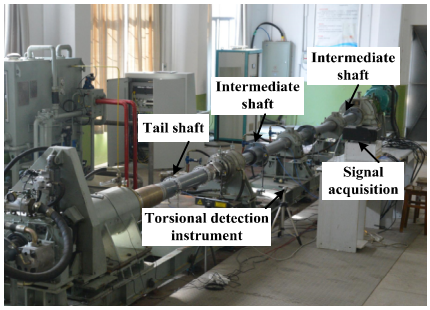

Fig. 3. The propulsion shaft experimental setup.

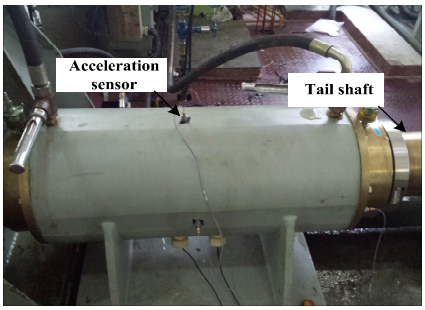

Fig. 4. Acceleration sensor placed on the tail bearing.

3.1 Idling vibration

In the idling vibration experiment (no excitation applied on the shaft), the acquisition and analysis of vibration signals were achieved by utilizing an acceleration sensor (Triaxial accelerometer sensor, type: B&K 4535-B-001) and a relevant vibration analyzer (Signal acquisition, type: PXIe-4499), including servo amplifiers, a signal acquisition card, a signal output device et cetera (Fig. 3). In order to ensure the accuracy of the test, the location of acceleration sensor was placed on the tail bearing which was close to the propeller, as shown in Fig. 4. A multichannel signal analyzer was used to collect the data and to obtain the vibration information in the time domain and frequency domain simultaneously.

The experimental setup allowed the propulsion shaft to rotate at various speeds. The maximum rotational speed of the shaft was designed to be about 550 revolutions per minute (rpm). In order to minimize the experimental error, the maximum rotational speed was defined close to 550 rpm. Thus, the experimental program of the dynamic response defines the rotational speed as 60 rpm, 100 rpm, 160 rpm, 260 rpm and 360 rpm (torsional detection instrument, type: B&K 2523 and Rotational speed sensor, type: B&K MM0024). The natural frequency and the ultimate deformation of the coupled vibrations were measured under the abovementioned five rotational speeds.

3.2 Loading vibration

In the loading vibration experiment, the transverse force was applied by the water hydraulic system installed between

Table 1. Properties of the propulsion shaft.

Property	Value
Length L	9.6 m
Diameters d	0.14-0.16 m
Density ρ	7850 kg/m^3
Elastic modulus E	210 GPa
Shear modulus G	77 GPa
Passion ratio v	0.3
Rotational speed ω	60-360 rpm

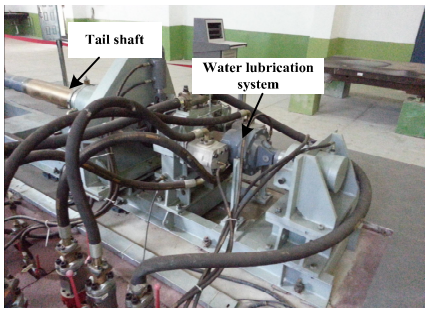

Fig. 5. The water lubrication system for the loading condition.

the tail bearing and the propeller (Fig. 5). The water hydraulic exciters in horizontal direction was used to simulate the excitation of the hull deformation. Mechanical sensors were installed on the exciters to monitor and control the magnitude of the force. In order to avoid shaft damage induced by excessive stresses, the value of transverse stress σ was set as 3.0 MPa to represent the linear deformation.

4. Numerical simulation

FEA was universally recognized as the most important technological breakthrough in the field of structural analysis and was widely used in the design and analysis of complex ship structures [19]. In this study, the FEA software ANSYS was employed to generate a computational protocol to simulate the coupled vibration experimental setup.

The rotational speed of numerical simulation was defined as the same as used in the experiment. The convergence criterion was set as that the simulation stopped when the maximum values of the residuals reached 0.001. The simulation results were obtained from the harmonic and transient analysis. The natural frequencies and ultimate deformations of all nodes in the coupled FEA model were also obtained.

4.1 Model construction

The finite element model of the shaft system was constructed using the solid element SOLID45, which is defined by eight nodes (three degrees of freedom at each node). The propeller was simulated by MASS21 element, which is a point element with six degrees of freedom. The mass of MASS21

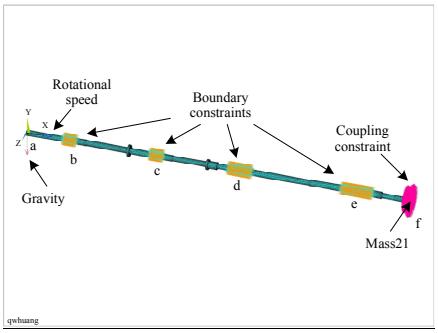

Fig. 6. The finite element model with boundary conditions.

was defined to be equal to the forces caused by the flow field around the propeller.

In order to ensure the accuracy of simulation results, the geometric and material properties of the model were set consistent with those used in the experiment. The detailed modeling input are listed in Table 1.

It was noticed that a reasonable mesh can reduce the number of element and/or nodes and shorten the calculation time without compromising the accuracy. Therefore, a mapped tetrahedral mesh pattern was employed for all the computational model, resulting in 28963 elements and 7354 nodes.

4.2 Boundary conditions

The boundary conditions applied in the FEA model were kept high consistent with the experiment setup, the boundary conditions, including displacement constraints, rotation constraints and coupling constraint. Fig 6 shows the meshed model with boundary conditions.

Specifically, the displacement constraints were set in the longitudinal direction, i.e. along the direction of the shaft. The rotation constraints were set in the radial direction, i.e. along with the rotational direction of the shaft. Both constraints were defined at the outer edge of the bearings (position b, c, d and e in Fig. 6) to simulate the supporting effects on the shaft. The coupling constraint was applied on the propeller, with the nodes in the cross section of element MASS21 being selected to couple with the solid elements of the same section (position f in Fig. 6). Moreover, the gravitational acceleration and the rotational speed were added to the simulated model (position a in Fig. 6).

In the simulation of the loading vibration, the loading condition was represented by transverse force. The value and position of the transverse loading in the coupled FEA model were consistent with those of the experiments. The transverse force N can be replaced by the stress σ according to the following formula:

$$\sigma = \frac{M}{W_z} \text{ and } M = N * L \tag{11}$$

where M is the bending moment, L is the length, W_z is the

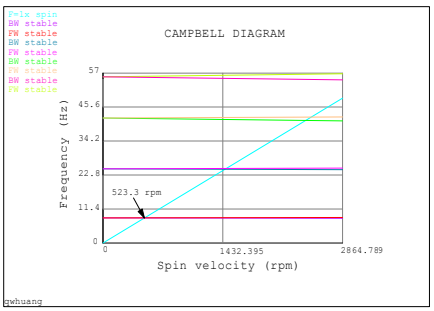

Fig. 7. The Campbell diagram of the critical speeds of the coupled FEA model (FW and BW are forward and backward whirl).

section modulus in bending, and $W_z = \pi d^3/32$. Thus, the transverse force is $N = W_z * \sigma / L$, which was applied to the model and the force vibration response were calculated.

4.3 Critical speeds analysis

Reliability of the shaft can be improved by defining a reasonable rotational speed [20]. To ensure that the state of shaft is stable for the defined rotational speeds, a critical speeds analysis was carried out using the Campbell diagram (Fig. 7), which showed the critical speeds (intersection points where the rotational speeds line crosses the curves) of all modes.

The result showed that the critical speeds of the first and second order are about 523.3 rpm and are much smaller than those of other orders. Therefore, the minimal critical speed was much larger than the maximum rotational speed (360 rpm) used in the experiment and simulation. Moreover, the forward and backward whirl of the eight orders were stable. Thus, the Campbell diagram confirmed that defined maximum rotational speed is reasonable.

5. Results and discussion

The dynamic parameters which describe the dynamic characteristic of a manipulator are important for control algorithms, system dynamic characteristic and precision and reliability [21, 22]. Therefore, the dynamic response including harmonic and transient analysis were obtained for both experimental and numerical methods. Harmonic response analysis is used to determine the steady-state response, i.e. the natural frequencies of structures, while the transient analysis provides information of the maximum displacement and stress of structures in the time domain.

5.1 Harmonic analysis

The results in Fig. 8 are the harmonic response of transverse vibration under idling condition, over a range of rotational speeds. The experimental transverse frequency ranges from 92.5 Hz to 130.6 Hz while the simulated results remains 116.3 Hz at different rotational speed. The results indicate that the natural frequency of transverse direction does not change significantly with the rotational speeds.

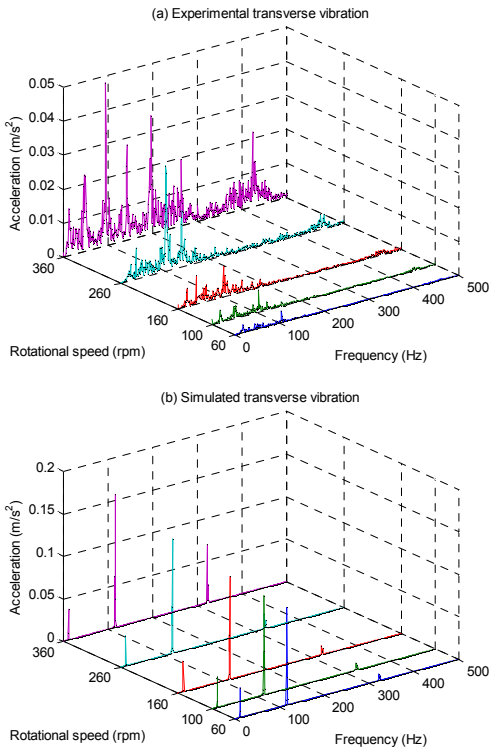

Fig. 8. Harmonic analysis of transverse vibration for idling condition: (a) Experimental results; (b) simulation results.

Results in Fig. 9 are the harmonic responses of longitudinal vibration under idling condition at different rotational speeds. The experimental longitudinal frequency ranges from 61.6 Hz to 68.5 Hz while the simulated frequency is 54.6 Hz. The results indicate that similar to the transverse vibration, the natural frequency of longitudinal direction shows little change with the rotational speeds. Furthermore, the amplitude of the natural frequencies increases with the increasing rotational speed.

5.2 Transient analysis

Fig. 10 shows the results of the transient responses of transverse vibration under idling condition for different rotational speeds. From the experimental results, it has been found that the minimal transverse acceleration is 0.10 m/s^2 (rotational speed = 60 rpm) and the maximum acceleration is 0.49 m/s^2 (rotational speed = 360 rpm). In comparison, the simulation results show that the accelerations range from 0.10 m/s^2 to 0.55 m/s^2.

The results of the transient responses of longitudinal vibration for the idling condition can be seen in Fig. 11. The experimental data indicate that the minimal longitudinal acceleration is 0.03 m/s^2 at 60 rpm and the maximum acceleration is 0.16 m/s^2 at 360 rpm, while the numerical model predicts that the accelerations range from 0.03 m/s^2 to 0.12 m/s^2.

It is found that the maximum amplitude of the coupled

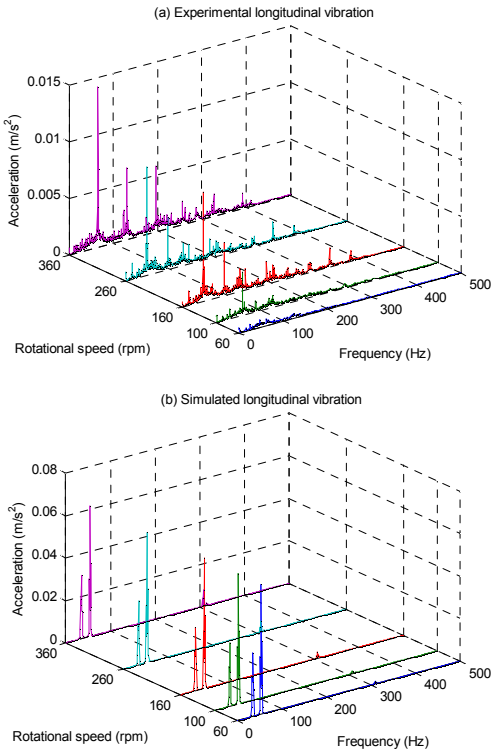

Fig. 9. Harmonic analysis of longitudinal vibration for idling condition: (a) Experimental results; (b) simulation results.

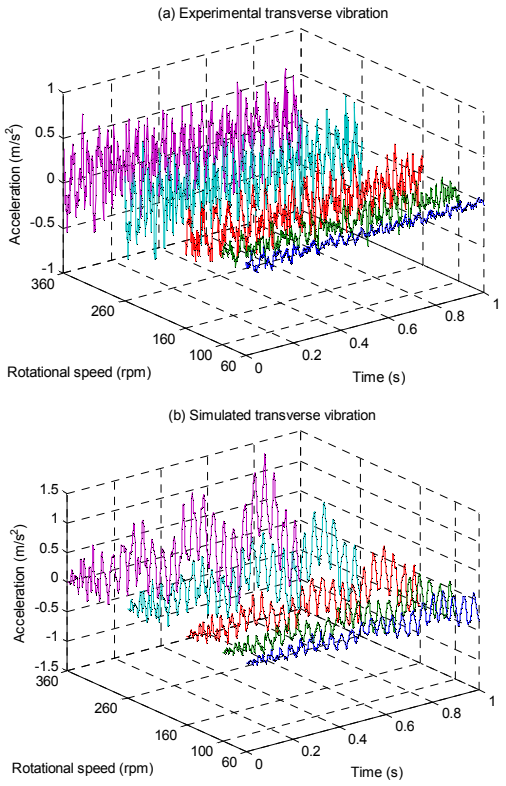

Fig. 10. Transient analysis of transverse vibration for idling condition: (a) Experimental results; (b) simulation results.

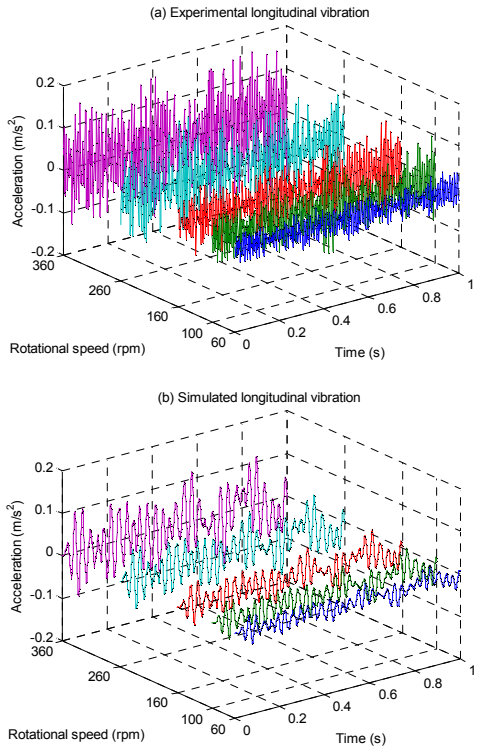

Fig. 11. Transient analysis of longitudinal vibration for idling condition: (a) Experimental results; (b) simulation results.

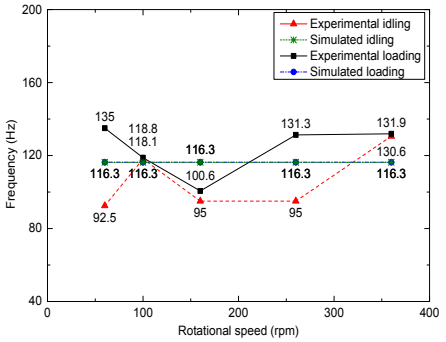

Fig. 12. The comparison of transverse harmonic results between experimental and simulation results for idling and loading conditions.

transverse and longitudinal vibration increases with increasing rotational speed for both experiment and simulation, which is in consistency with the harmonic analysis.

5.3 Comparison between idling and loading vibration

The abovementioned Figs. 8-11 indicate that there is a fiducial interval for the idling vibration performance between the experiment and the simulation. Similar behavior was obtained for the loading condition. In order to investigate the deviation caused by experimental tests, the influence on vibration response will be discussed. The comparison of the experimental and simulation results of the coupled vibration for idling and loading conditions are presented in Figs. 12-15.

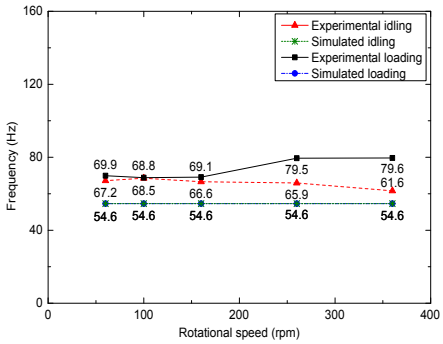

Fig. 13. The comparison of longitudinal harmonic results between experimental and simulation results for idling and loading conditions.

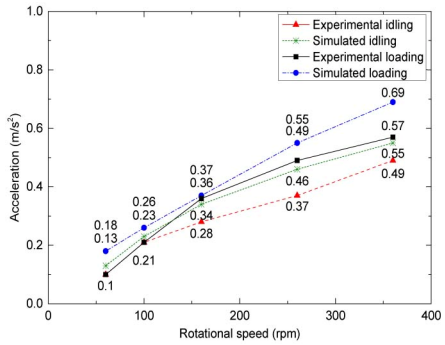

Fig. 14. The comparison of transverse transient results between experimental and simulation results for idling and loading conditions.

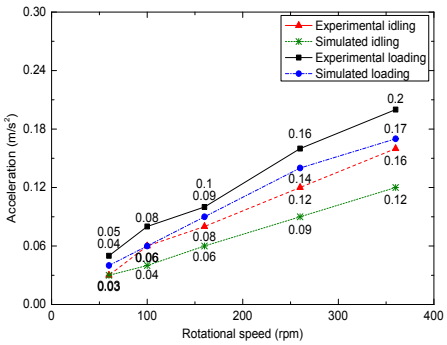

Fig. 15. The comparison of longitudinal transient results between experimental and simulation results for idling and loading conditions.

Fig. 12 reveals that the transverse frequency is independent of the rotational speeds in a harmonic analysis. The experimental frequency is in the range of 92.5 Hz to 130.6 Hz for the idling condition, and 100.6 Hz to 135.0 Hz for the loading condition. The simulated frequency remains 116.3 Hz for both conditions at different rotational speeds.

Similarly, the longitudinal frequency is also found to be independent of the rotational speeds in the harmonic analysis (Fig. 13), with the experimental frequency ranges from 61.6 Hz to 68.5 Hz for the idling condition, and 68.8 Hz to 79.6 Hz under the loading condition, while the simulated frequency remains constant (54.6 Hz) at different rotational speeds.

However it is interesting to notice that the transverse (Fig. 14) and longitudinal (Fig. 15) accelerations increases with increasing rotational speed in a transient analysis. For the transverse responses, in the case of idling condition, as the rotational speed increases, the experimental transverse accelerations increases from 0.10 m/s^2 to 0.49 m/s^2 while the simulation frequency changes from 0.13 m/s^2 to 0.55 m/s^2. Regarding the loading condition, the experimental transverse acceleration increases range from 0.10 m/s^2 to 0.57 m/s^2 and the simulation result ranges from 0.18 m/s^2 to 0.69 m/s^2, over a range of rotational speeds.

For the longitudinal direction, under idling condition, the experimental longitudinal acceleration increases from 0.03 m/s^2 to 0.16 m/s^2 with the rotational speed whereas the simulated acceleration increases from 0.03 m/s^2 to 0.12 m/s^2. In terms of the loading condition, the longitudinal acceleration increments with speed obtained from the experiment and the simulation are 0.05 m/s^2 to 0.20 m/s^2 and 0.04 m/s^2 to 0.17 m/s^2, respectively.

It is considered that during the experimental measurement, the propeller shaft experiences the frictional force induced by oil film resistance, stern bearing, damping, mechanical noise and other influence factor, which was not included in the FEA model. As a result, small deviations for the natural frequency and maximum acceleration between experimental and simulation results are observed.

As it mentioned in Eqs. (4) and (5), the increasing rotational speed can increase the corresponding u" and v", and then the acceleration $\ddot{u}$ and $\ddot{v}$ of coupled vibrations increase, as shown in Eqs. (9) and (10). This can explain the acceleration change larger with greater rotational speed, and also prove that the acceleration for loading condition is severer than idling condition. Moreover, while the experimental results show increasing accelerations with increasing rotational rates, some simulated results appear to slightly under predict the acceleration in comparison to the experimental results, especially at greater rotational speeds.

6. Conclusions

In this paper, a finite element method was proposed to study the coupled transverse and longitudinal vibration performances of the marine propulsion shaft system under both the idling and loading condition.

In general, the numerical simulation results are found to agree well with the experimental measurements over the range of investigated rotational speeds (60-360 rpm). The accuracy of the coupled finite element model is therefore validated. The results also indicate that the maximum transverse and longitudinal accelerations increase with increasing rotational speeds. And loading condition enlarge the acceleration by a comparison with idling condition. While the natural frequencies of the coupled vibrations are found to be independent of the rotational speed.

Furthermore, the transverse and longitudinal vibrations are

interacting with each other. It is therefore vital to not only consider the vibration frequency along an individual direction of the shaft but also to minimize the interaction/coupling effect among vibrations in different directions. The proposed FEA model is capable of predicting and quantifying the behaviour of a coupled maintenance of the marine propulsion shaft system.

Acknowledgment

This work is supported by the State Key Program Grant of National Natural Science Foundation of China (No. 5113 9005), China.

References

[1] L. Qin et al., Shaft power measurement for marine propulsion system based on magnetic resonances, *IEICE Electronics Express*, 2 (2012) 49-55.

[2] L. Murawski, Some aspects of torsional vibration analysis methods of marine power transmission systems, *Journal of Polish CIMAC*, 7 (2) (2012) 175-182.

[3] G. B. Zhang et al., Propeller excitation of longitudinal vibration characteristics of marine propulsion shafting system, *Shock and Vibration* (2014) 413592 (19 pp).

[4] R. Warikoo and M. R. Haddara, Analysis of propeller shaft transverse vibrations, *Marine Structures*, 5 (1992) 255-279.

[5] M. G. Parsons, J. Srinivas and V. Raju, Mode coupling in torsional and longitudinal shafting vibration, *Marine Technology*, 20 (1983) 257-271.

[6] X. P. Yan et al., Study on coupling dynamical theory for interaction of propulsion system and hull of large ships: a review, *Journal of Ship Mechanics*, 17 (4) (2013) 439-449.

[7] L. Murawski and A. Charchalis, Simplified method of torsional vibration calculation of marine power transmission system, *Marine Structure*, 39 (2014) 335-349.

[8] A. Yucel and A. Arpaci, Free and forced vibration analyses of ship structures using the finite element method, *Journal of Marine Science and Technology*, 18 (2013) 324-338.

[9] Y. M. Huang and C. D. Horng, Analysis of torsional vibration systems by the extended transfer matrix method. Transactions of the ASME, *Journal of Vibration and Acoustics*, 121 (2) (1999) 250-255.

[10] M. O. Jang et al., A study on the coupled torsional-axial vibration of marine propulsion shafting system using the energy method, *Journal of the Korean Society of Marine Engineers*, 3 (2004) 482-492.

[11] J. S. Wu et al., Computer method for torsion-and-flexure-coupled forced vibration of shafting system with damping, *Journal of Sound and Vibration*, 180 (3) (1995) 417-435.

[12] M. A. Rao et al., Coupled torsional-lateral vibration analysis of geared shaft systems using mode synthesis, *Journal of Sound and Vibration*, 261 (2003) 359-364.

[13] S. I. Paul, The interaction between diesel engine, ship and propeller during maneuvering, *Ph.D. Dissertation,* Delft: Delft University of Technology (2005).

[14] L. Murawski, Axial vibrations of a propulsion system taking into account the couplings and the boundary conditions, *Journal of Marine Science and Technology*, 9 (2004) 171-181.

[15] L. Chris, *Shaft alignment and powertrain vibration*, ABS (2011).

[16] Q. W. Huang et al., Vibration analysis of marine propulsion shafting by the coupled finite element method, *Journal of Vibroengineering*, 17 (2015) 3392-3403.

[17] D. Oguamanam, Free vibration of beams with finite mass rigid tip load and flexural-torsional coupling, *International Journal of Mechanic Science*, 45 (2003) 963-979.

[18] X. Xu, Research on the theory and experiment of coupled vibration for marine complex propulsion shafting, *Ph.D. Dissertation,* Wuhan University of Technology (2012).

[19] T. R. Lin, J. Pan, P. J. O'Shea and C. K. Mechefske, A study of vibration and vibration control of ship structures, *Marine Structures*, 22 (2009) 730-743.

[20] Y. Tian et al., Critical speeds of a high speed motor with different supports and rotor assembly, *Journal of Vibration and Shock*, 32 (2013) 24-29.

[21] C. X. Zhu, J. Wang, Z. W. Chen and B. Liu, Dynamic characteristic parameters identification analysis of a parallel manipulator with flexible links, *Journal of Mechanical Science and Technology*, 28 (12) (2014) 4833-4840.

[22] R. Zhou, W. Zhang and J. W. Zu, Analysis on nonlinear dynamics of a thin-plate workpiece in milling process with cutting force nonlinearities, *Journal of Mechanical Science and Technology*, 28 (7) (2014) 2511-2526.

Qianwen Huang is currently a Ph.D. candidate in Wuhan University of Technology, China and a visiting academic in University of Southampton, UK. His research interests include vibration mechanics, computational modeling and dynamical measurement.